2006 ERSD Annual Report
DOE-BER Environmental Remediation Sciences Project #90230

Mineralogic Residence and Desorption Rates of Sorbed ^{90}Sr in Contaminated Subsurface Sediments: Implications to Future Behavior and In-Ground Stability

PIs: John M. Zachara[1]
Co-PIs: Jim P. McKinley[1], S. M. Heald[1,2], Chongxuan Liu[1], and Peter C. Lichtner[3]
[1]Pacific Northwest National Laboratory, Richland, WA
[2]Argonne National Laboratory, Argonne, IL
[3]Los Alamos National Laboratory, Los Alamos, NM

Research Objectives:

The project is investigating the adsorption/desorption process of ^{90}Sr in coarse-textured pristine and contaminated Hanford sediment with the goal to define a generalized reaction-based model for use in reactive transport calculations. While it is known that sorbed ^{90}Sr exists in an ion exchangeable state, the mass action relationships that control the solid-liquid distribution and the mineral phases responsible for adsorption have not been defined. Many coarse-textured Hanford sediment display significant sorptivity for ^{90}Sr, but contain few if any fines that may harbor phyllosilicates with permanent negative charge and associated cation exchange capacity. Moreover, it is not known whether the adsorption-desorption process exhibits time dependence within context of transport, and if so, the causes for kinetic behavior. Consequently, the research objectives are:

- To develop a generalized multi-component ion exchange model for ^{90}Sr adsorption-desorption on Hanford sediments based on experimental measurements.
- To identify important mineral phases that adsorb ^{90}Sr through investigations of ^{90}Sr-contaminated subsurface sediments from multiple Hanford locations.
- To ascertain whether ^{90}Sr desorption follows ion exchange mass action relationships or exhibits retarded kinetic behavior.

Research Progress and Implications:

An ion exchange model has been developed through study of deep vadose zone sediments from the S-SX tank farm in Hanford's 200 A plateau, and Columbia River Corridor aquifer sediments from the 100 N Sr-plume. Calcium was used as the reference cation because of the presence of minor calcite in both sediments that fixes Ca^{2+} aqueous activity. Binary exchange isotherms involving Ca-Mg, Ca-Na, and Ca-Sr were measured at three ionic strengths. These were analytically intensive, and involved the characterization of the aqueous and exchanger-phase composition at equilibrium. The exchanger phase composition was characterized by ammonium chloride extraction, and the sum of the extracted cations for each sediment defined a constant CEC (e.g., Figure 1.). The resulting exchange isotherms were generally linear for each ion relative to Ca^{2+}. Eighteen isotherms (e.g., three each for Na^+, Mg^{2+}, and Sr^{2+}, for two sediments) were fit to yield a consistent set of Vanselow selectivity coefficients. The exchange coefficients showed small differences between sediments from the 200 A vadose zone and the river corridor alluvial aquifer. The applicability of these exchange constants to describe the reactive transport of ^{90}Sr was evaluated in a series of column experiments with different

Ca^{2+}/Na^+ ratios and Sr^{2+} concentration. Predicted and measured ^{90}Sr breakthrough curves compared well, except for those at the highest ionic strength (0.1 mol/L).

^{90}Sr-contaminated sediments were obtained from a core collected proximate to Tank B-110 in Hanford's B tank farm. The subsurface sediments were coarse and contained few fines. The core intersected a HLW plume at 26 m where significant adsorbed ^{90}Sr was present. Thin sections were made from the sediments and these were subjected to high resolution digital autoradiography (Figure 3) that allowed the identification of ^{90}Sr-containing mineral domains in multi-component, basaltic mineral fragments. Such domains were unexpected and implied the presence of an intragrain mineral phase with significant CEC that had formed from the weathering of basaltic glass.   The ^{90}Sr-containing mineral domains were analyzed by TEM and SEM microbeam techniques to determine their elemental composition and mineral structure. They appeared to be a saponites, e.g. ferrous iron containing phyllosilicates.

The contaminated sediments were placed in electrolytes of variable composition and ionic strength to determine if sorbed, HLW ^{90}Sr was desorbable. The experiments tracked the rate of ^{90}Sr release with time.. Almost no ^{90}Sr desorbed to deioized water or low concentration Na-electrolyte (Figure 4). However significantly more ^{90}Sr was desorbed as the ionic strength was increased, and when divalent Ca was present. These results were consistent with an ion exchange adsorption state for approximately 80% of the sorbed ^{90}Sr. Acid extraction of the sediments after contact with high ionic strength electrolyte indicated that 20% of contaminant ^{90}Sr was co-precipitated with calcite. Through a somewhat involved modeling process, the desorption results could be well described by a combination of ion exchange and calcite dissolution.

Planned Activities:

The project ended on Sept. 30, 2006. No further research activities are planned, although a final publication will be completed in FY 07 with carry-over funding.

Information Access:

Publications

McKinley, J. P., J. M. Zachara, S. C. Smith, and C. Liu. 2006. Cation exchange reactions controlling desorption of $^{90}Sr^{2+}$ from coarse-grained contaminated sediments from the Hanford formation, Washington. *Geochimica et Cosmochimica Acta* (Accepted).

Steefel, C. I., P. C. Lichtner, J. M. Zachara, and S. C. Smith. 2006. A generalized ion and isotopic exchange model for Sr^{2+} and $^{90}Sr^{2+}$ adsorption to subsurface sediments and its application to reactive transport. *Geochimica et Cosmochimica Acta* (Submitted).
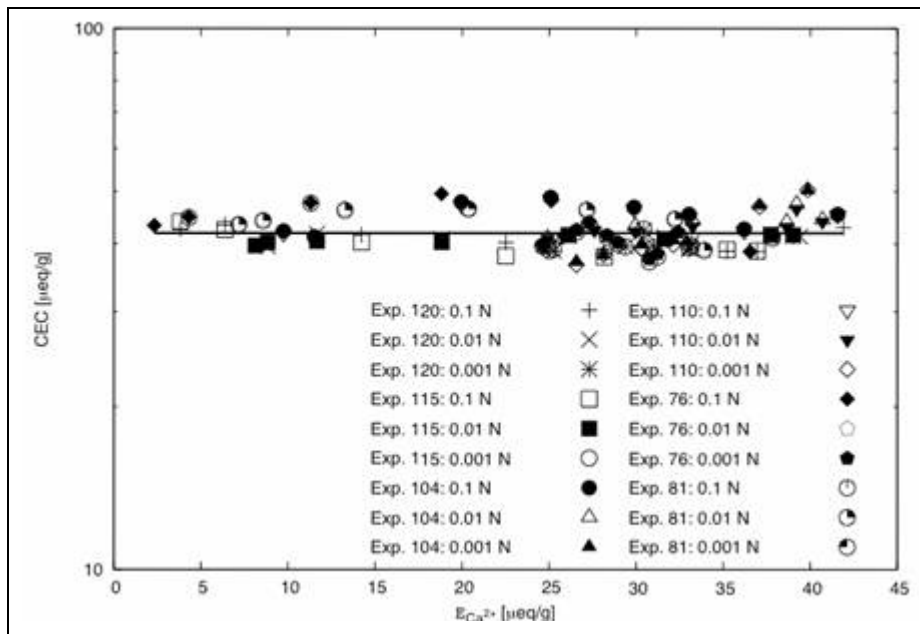
Figure 1. The sum of exchangeable cations displaced from the 200 A fine sand composite in various experiments (HFSC) by ammonium chloride. The average defines the cation exchange capacity (CEC).
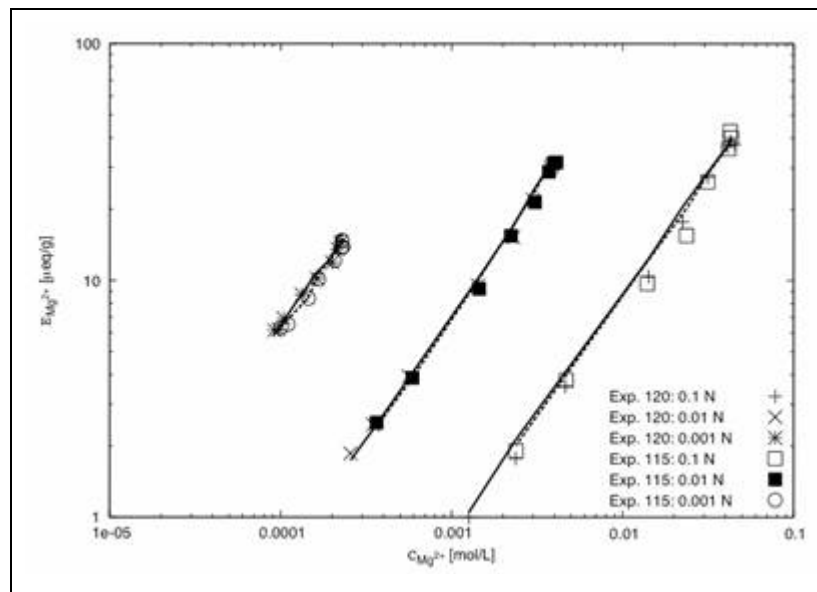
Legend (Figure 1):
Exp. 120: 0.1 N
Exp. 120: 0.01 N
Exp. 120: 0.001 N
Exp. 115: 0.1 N
Exp. 115: 0.01 N
Exp. 115: 0.001 N
Exp. 104: 0.1 N
Exp. 104: 0.01 N
Exp. 104: 0.001 N
Exp. 110: 0.1 N
Exp. 110: 0.01 N
Exp. 110: 0.001 N
Exp. 76: 0.1 N
Exp. 76: 0.01 N
Exp. 76: 0.001 N
Exp. 81: 0.1 N
Exp. 81: 0.01 N
Exp. 81: 0.001 N

Axes (Figure 1): CEC [μeq/g] vs $E_{Ca^{2+}}$ [μeq/g]

Figure 2. Ion exchange isotherms of Mg^{2+} on Ca^{2+} saturated fine sand composite. Three ionic strengths are represented. Isotherms for other ion pairs showed comparable linearity.
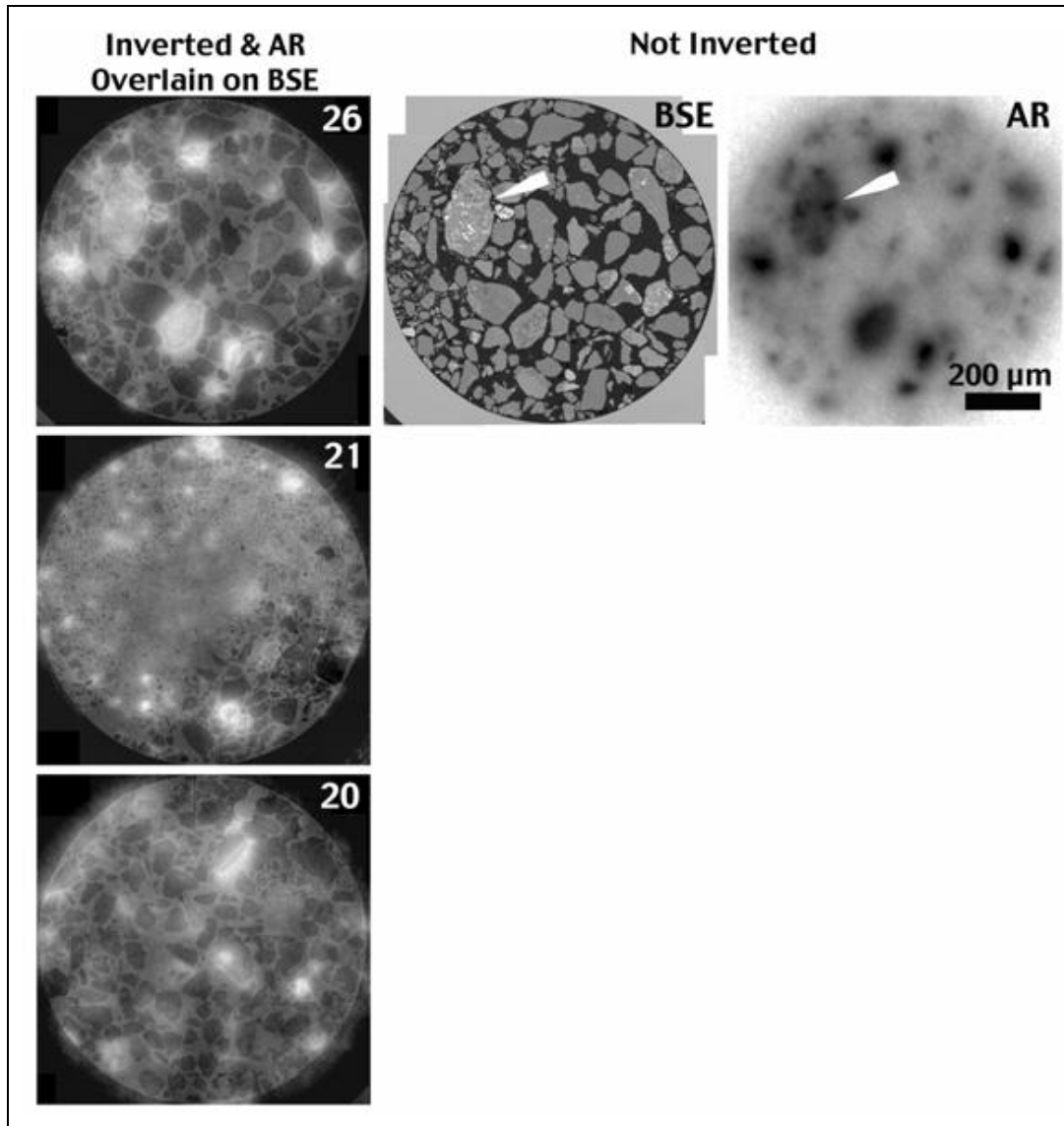
Legend (Figure 2):
Exp. 120: 0.1 N
Exp. 120: 0.01 N
Exp. 120: 0.001 N
Exp. 115: 0.1 N
Exp. 115: 0.01 N
Exp. 115: 0.001 N

Axes (Figure 2): $E_{Mg^{2+}}$ [μeq/g] vs $c_{Mg^{2+}}$ [mol/L]

Figure 3. Digital auto radiographs of three B-110 sediments overlain on backscattered electron micrographs (BSE) of the sediment thin sections. ^{90}Sr-containing regions are shown in white on the inverted images and in black on the images not inverted. The chemical composition and mineral structure of the ^{90}Sr-containing regions were mapped in detail.
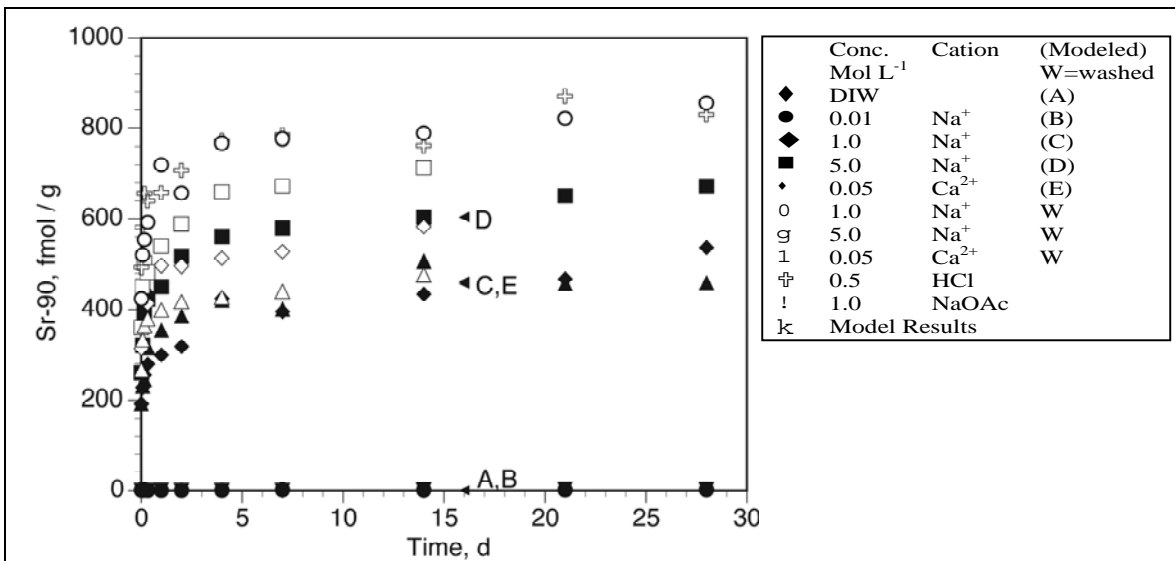
Figure 4. Desorption kinetics of ^{90}Sr from contaminated sediment B-110-26A in different electrolyte solutions. Ion exchange model predictions are labeled by A, B, C, D, and E. Details are presented in McKinley et al., (2006).